Contribution from the Department of Chemistry-0506, University of California at San Diego, La Jolla, California 92093-0506, School of Chemical Sciences, University of Illinois, Urbana, Illinois 61801, Department of Chemistry, University of Louisville, Louisville, Kentucky 40292, and Microcalorimetry Research Center, Faculty of Science, Osaka University, Toyonaka, Osaka 560, Japan

Subtle Effects of Solvate Molecules on the Rate of Intramolecular Electron Transfer of Mixed-Valence Complexes in the Solid State†

Ho G. Jang,[1] Richard J. Wittebort,*[,2] Michio Sorai,*[,3] Yuki Kaneko,[3] Motohiro Nakano,[3] and David N. Hendrickson*[,4]

Received October 30, 1991

The microscopic nature of the valence-detrapping phase transition of $[Fe_3O(O_2CCH_3)_6(4\text{-Me-py})_3](CHCl_3)$ (**2**) is studied. The constant-pressure heat capacity of a 16.3703-g sample of **2** in the 14–300 K range is presented. An apparently first-order phase transition with two C_p peaks at 93.48 and 95.04 K was observed. After correction for the normal heat capacity, the total entropy gain for the phase transition was found to be $\Delta S = 17.18 \pm 1.42$ J K^{-1} mol^{-1}, which is close to $\Delta S = R \ln 8$ (=17.29 J K^{-1} mol^{-1}). Isostructural $[Fe_3O(O_2CCH_3)_6(py)_3](CHCl_3)$ (**1**) has been reported to have a "double-peaked" phase transition at ~208 K with $\Delta S = 28.10 \pm 0.44$ J K^{-1} mol^{-1}, which is close to $\Delta S = R \ln 32$ (=28.82 J K^{-1} mol^{-1}). The valence-detrapping phase transition in both cases involves each Fe_3O complex converting from being statically trapped in one vibronic state to dynamically interconverting between four vibronic states. For both **1** and **2**, this contributes $\Delta S = R \ln 4$. Even though it has been reported that the $CHCl_3$ solvate molecules in **1** cooperatively convert from being static in one lattice position to jumping between eight positions in the phase transition, the $CHCl_3$ molecules in **2** only start jumping between two positions where the C–H vector is pointing either up or down along the *c* axis (C_3 axis). For **2**, the $CHCl_3$ solvate molecules only contribute $\Delta S = R \ln 2$. The nature of the motion of the chloroform solvate molecule is examined in detail by employing solid-state ^{2}H NMR spectroscopy on magnetically oriented crystalline samples of $[Fe_3O(O_2CCH_3)_6(4\text{-Me-py})_3](CDCl_3)$. In these crystals, the C–D vector is jumping between positions on a cone axially symmetric about the C_3 axis. At 290 K, this cone is ~18° off the C_3 axis. A decrease in the temperature reduces this angle to 10° at 145 K and presumably 0° below the ~94 K phase transition. Thus, for complex **2** at the ~94 K phase transition the *c* axis of the crystal is too small to permit the chloroform C–H vector to precess about the *c* axis (C_3 axis). The cooperative motion of the $CHCl_3$ molecules in **2** at ~94 K involve only a head-to-tail motion with the C–H vector on the *c* axis.

Introduction

The influence of the environment on the rate of electron transfer between two transition metal ions is not well characterized.[5] For example, the electronic structure of a redox pair such as $Fe(H_2O)_6^{2+}$···$Fe(H_2O)_6^{3+}$ in water is probably vibronic.[6] Vibrational modes associated with the surrounding water and/or cation structure could modulate the rate of electron transfer. In this same manner, vibronic interactions associated with redox sites in metalloproteins could lead to these redox sites being switched on or off for electron transfer by the onset of environmental dynamics. A conformational change in a metalloprotein could lead to an amino acid residue and/or water structure about the redox site becoming dynamic. This possibility has been examined[7] in detail for cytochrome *c*, which is the best characterized member of a group of over 50 metallo- and flavoproteins which constitute the mitochondrial respiratory electron-transport chain. Williams et al.[7] suggested that the phenyl moiety of one or more of three phenylalanine and tyrosine residues which are near the heme group flips at a rate in excess of $\sim 10^4$ s^{-1}. This motion could couple with the heme site to activate it to a vibrational level from which tunneling to and from the heme site would be facilitated. For the reactions of cytochrome *c* with its physiological redox partners, the rate of electron transfer is in the range 10^2–10^4 s^{-1}.

The study of intramolecular electron-transfer events in mixed-valence metal complexes[8] *in the solid state* can provide insight into whether the onset of motion of nearby solvate molecules influences the rate of intramolecular electron transfer. The nature of the solvate molecule S in mixed-valence $[Fe_3O(O_2CCH_3)_6(L)_3]S$, where L is (substituted) pyridine, has been shown[9] to affect dramatically the rate of electron transfer in the $Fe^{II}Fe^{III}_2$ complex. In a series of isostructural complexes where only S is changed from one complex to another, the temperature at which a given complex valence detraps is dependent upon S. This sensitivity is a reflection of the fact that the lowest-energy states of $[Fe_3O(O_2CCH_3)_6(L)_3]S$ are vibronic, and as a result these complexes are very sensitive to their environment. In other words, the electronic coordinates of these $Fe^{II}Fe^{III}_2$ complexes are strongly coupled to certain vibrational coordinates. In the intramolecular electron-transfer process, the complex is involved in a relatively large amplitude vibrational motion to adjust the Fe^{II} environment to that of a Fe^{III} ion and vice versa. Even weak van der Waals interactions with a nearby solvate molecule in the crystal can influence the rate of electron transfer in the $Fe^{II}Fe^{III}_2$ complex. Such a pronounced sensitivity of rate of electron transfer to environment has also been noted[10] for salts of $Fe^{II}Fe^{III}$ biferrocenium cations. Very recently

† The calorimetric part of this paper corresponds to Contribution No. 5 from the Microcalorimetry Research Center, Osaka University.

(1) University of Illinois.
(2) University of Louisville.
(3) Osaka University.
(4) University of California at San Diego.
(5) Recent reviews: (a) DeVault, D. *Quantum-Mechanical Tunnelling in Biological Systems*, 2nd ed.; Cambridge University Press: Cambridge, U.K., 1984. (b) Cannon, R. D. *Electron Transfer Reactions*; Butterworths: Boston, MA, 1980. (c) Marcus, R. A.; Sutin, N. *Biochim. Biophys. Acta* **1985**, *811*, 265. (d) Mikkelsen, K. V.; Ratner, M. A. *Chem. Rev.* **1987**, *87*, 113.
(6) (a) Jortner, J.; Bixon, M. *J. Chem. Phys.* **1988**, *88*, 167. (b) Tembe, B. L.; Friedman, H. L.; Newton, M. D. *J. Chem. Phys.* **1982**, *76*, 1490.
(7) Williams, G.; Moore, G. R.; Williams, R. J. P. *Comments Inorg. Chem.* **1985**, *4*, 55–98.
(8) Recent reviews: (a) Day, P. *Int. Rev. Phys. Chem.* **1981**, *1*, 149. (b) Brown, D. B., Ed. *Mixed-Valence Compounds, Theory and Applications in Chemistry, Physics, Geology and Biology*; Reidel Publishing Co.: Boston, MA, 1980. (c) Creutz, C. *Prog. Inorg. Chem.* **1983**, *30*, 1. (d) Richardson, D. E.; Taube, H. *Coord. Chem. Rev.* **1984**, *60*, 107.
(9) (a) Jang, H. G.; Geib, S. J.; Kaneko, Y.; Nakano, M.; Sorai, M.; Rheingold, A. L.; Montez, B.; Hendrickson, D. N. *J. Am. Chem. Soc.* **1989**, *111*, 173. (b) Kaneko, Y.; Nakano, M.; Sorai, M.; Jang, H. G.; Hendrickson, D. N. *Inorg. Chem.* **1989**, *28*, 1067. (c) Oh, S. M.; Wilson, S. R.; Hendrickson, D. N.; Woehler, S. E.; Wittebort, R. J.; Inniss, D.; Strouse, C. E. *J. Am. Chem. Soc.* **1987**, *109*, 1073. (d) Woehler, S. E.; Wittebort, R. J.; Oh, S. M.; Kambara, T.; Hendrickson, D. N.; Inniss, D.; Strouse, C. E. *J. Am. Chem. Soc.* **1987**, *109*, 1063. (e) Woehler, S. E.; Wittebort, R. J.; Oh, S. M.; Hendrickson, D. N.; Inniss, D.; Strouse, C. E. *J. Am. Chem. Soc.* **1986**, *108*, 2938. (f) Hendrickson, D. N.; Oh, S. M.; Dong, T.-Y.; Kambara, T.; Cohn, M. J.; Moore, M. F. *Comments Inorg. Chem.* **1985**, *4*, 329. (g) Sorai, M.; Kaji, K.; Hendrickson, D. N.; Oh, S. M. *J. Am. Chem. Soc.* **1986**, *108*, 702. (h) Oh, S. M.; Hendrickson, D. N.; Hassett, K. L.; Davis, R. E. *J. Am. Chem. Soc.* **1985**, *107*, 8009.
(10) (a) Dong, T.-Y.; Cohn, M. J.; Hendrickson, D. N.; Pierpont, C. G. *J. Am. Chem. Soc.* **1985**, *107*, 4777. (b) Cohn, M. J.; Dong, T.-Y.; Hendrickson, D. N.; Geib, S. J.; Rheingold, A. L. *J. Chem. Soc., Chem. Commun.* **1985**, 1095. (c) Dong, T.-Y.; Hendrickson, D. N.; Iwai, K.; Cohn, M. J.; Rheingold, A. L.; Sano, H.; Motoyama, I.; Nakashima, S. *J. Am. Chem. Soc.* **1985**, *107*, 7996. (d) Dong, T.-Y.; Hendrickson, D. N.; Pierpont, C. G.; Moore, M. F. *J. Am. Chem. Soc.* **1986**, *108*, 963. (e) Moore, M. F.; Wilson, S. R.; Cohn, M. J.; Dong. T.-Y.; Mueller-Westerhoff, U. T.; Hendrickson, D. N. *Inorg. Chem.* **1985**, *24*, 4559. (f) Dong, T.-Y.; Kambara, T.; Hendrickson, D. N. *J. Am. Chem. Soc.* **1986**, *108*, 4423. (g) Dong, T.-Y.; Kambara, T.; Hendrickson, D. N. *J. Am. Chem. Soc.* **1986**, *108*, 5857. (h) Sorai, M.; Nishimori, A.; Hendrickson, D. N.; Dong, T.-Y.; Cohn, M. J. *J. Am. Chem. Soc.* **1987**, *109*, 4266. (i) Kambara, T.; Hendrickson, D. N.; Dong, T.-Y.; Cohn, M. J. *J. Chem. Phys.* **1987**, *86*, 2362.

0020-1669/92/1331-2265$03.00/0

Table I. ^{57}Fe Mössbauer Fitting Parameters for $[Fe_3O(O_2CCH_3)_6(4\text{-Me-py})_3](CHCl_3)$[a]

	δ, mm/s[b]			ΔE_Q, mm/s			Γ, mm/s[c]			% area		
T, K	Fe^{III}	Fe^{av}	Fe^{II}	Fe^{III}	Fe^{av}	Fe^{II}	Fe^{III}	Fe^{av}	Fe^{II}	Fe^{III}	Fe^{av}	Fe^{II}
6	0.533 (1)		1.249 (1)	1.245 (1)		1.515 (2)	0.133 (2) 0.141 (2)		0.196 (2) 0.196 (2)	64.2 (1)		36.8 (1)
57	0.533 (1)		1.233 (2)	1.202 (2)		1.407 (4)	0.152 (2) 0.167 (2)		0.182 (4) 0.212 (4)	66.8 (1)		33.2 (1)
77	0.533 (1)		1.225 (2)	1.162 (2)		1.357 (4)	0.172 (2) 0.157 (2)		0.172 (4) 0.215 (4)	66.8 (1)		33.2 (1)
81	0.539 (1)	0.600 (9)	1.211 (2)	1.160 (2)	0.697 (9)	1.256 (3)	0.154 (2) 0.139 (2)	0.274 (6) 0.228 (6)	0.153 (3) 0.207 (6)	52.0 (1)	21.2 (4)	26.8 (1)
200		0.599 (1)			0.828 (1)			0.223 (1) 0.175 (1)			100 (1)	
298		0.555 (1)			0.767 (1)			0.146 (1) 0.146 (1)			100 (1)	

[a] Peaks were least-squares-fit to Lorentzian line shapes with equal areas for both components of a doublet; error in the last significant figure is given in parentheses. [b] Center shifts relative to Fe metal at room temperature. [c] Half-width at half-maximum listed in order of increasing velocity of the peak.

we reported[11] that changing from I_3^- to PF_6^- for the counteranion of the 1′,1‴-diiodobiferrocenium cation leads to a change from being valence detrapped (one doublet) at 4.2 K to being valence trapped at 350 K (two doublets) on the ^{57}Fe Mössbauer time scale.

This paper is concerned with a comparison of electron-transfer characteristics of $[Fe_3O(O_2CCH_3)_6(py)_3](CHCl_3)$ (**1**) and isostructural $[Fe_3O(O_2CCH_3)_6(4\text{-Me-py})_3](CHCl_3)$ (**2**), where py is pyridine and 4-Me-py is 4-methylpyridine. In both cases, there is one $CHCl_3$ above and one below each $Fe^{II}Fe^{III}_2$ complex in the crystal. By the use of solid-state ^{2}H NMR spectroscopy on oriented crystals, combined with heat capacity measurements and ^{57}Fe Mössbauer spectroscopy, it was shown[9a,b] for complex **1** that the $CHCl_3$ solvate experiences an onset of motion at just the same temperature at which the neighboring $Fe^{II}Fe^{III}_2$ complex begins interconverting between its vibronic states. Along the C_3 axis of the $R32$ space group, Fe_3O complexes and $CHCl_3$ solvate molecules occupy alternating sites of 32 symmetry. The C–H vector of the $CHCl_3$ points at the Fe_3O complex. The dynamics of the $CHCl_3$ involves the C–H vector jumping between four positions, one along the c axis and the other three positions equally spaced on a cone ~25° off the c axis. The presence of four positions (actually four up and four down) for the chloroform C–H vector was deduced[9a] from the X-ray results combined with solid-state ^{2}H NMR results. What is fascinating is that as the C–H chloroform vector moves between these four positions, the Fe_3O complex interconverts (i.e., electron transfer) between its four vibronic states ($Fe_a^{II}Fe_b^{III}Fe_c^{III}$, $Fe_a^{III}Fe_b^{II}Fe_c^{III}$, $Fe_a^{III}Fe_b^{III}Fe_c^{II}$, and an electronically delocalized state). In this paper, subtle and intriguing differences associated with the influence of solvate molecule motion will be documented for $[Fe_3O(O_2CCH_3)_6(4\text{-Me-py})_3](CHCl_3)$.

Experimental Section

^{57}Fe Mössbauer Spectroscopy. Variable-temperature spectra were obtained in vertical transmission geometry by using a constant-acceleration spectrometer which has been described before.[12] Computer fittings of the Mössbauer data to Lorentzian line shapes were carried out with a modified version of a previously reported computer program.[13] Isomer shift values are reported relative to iron foil at 298 K but are not corrected for the temperature-dependent second-order Doppler shift.

Heat Capacity Measurements. Heat capacities were measured with an adiabatic calorimeter[14] in the range 14–300 K. A calorimeter cell[15] made of gold-plated copper was loaded with 16.3703 g (0.017 4790 mol) of polycrystalline $[Fe_3O(O_2CCH_3)_6(4\text{-Me-py})_3](CHCl_3)$ with buoyancy correction assuming a density of 1.34 g cm^{-3}. A small amount of helium gas was sealed in the cell to aid in heat transfer.

Solid-State ^{2}H NMR Spectroscopy. ^{2}H NMR spectra were obtained on a "homebuilt" 5.9-T spectrometer described previously.[16] The pulse sequence was a standard quadrupole echo sequence $[(90)_x\text{–}t\text{–}(90)_y\text{–}t\text{–}$observe] with t = 30–50 μs and a 90° pulse width of 2.7 μs. To prepare the magnetically oriented sample, ~20 small crystals of $[Fe_3O(O_2CCH_3)_6(4\text{-Me-py})_3](CDCl_3)$ were suspended in fluid eicosane (mp = 38 °C) at 50 °C while the crystals were oriented by the 5.9-T magnetic field. In the presence of the magnetic field, each small crystal turns so that the principal axis (c axis of the $R32$ symmetry crystal) of the magnetic susceptibility tensor of the crystal aligns parallel to the external magnetic field. After alignment was achieved, the hydrocarbon matrix was then slowly cooled to room temperature to form a solid block with the crystals embedded in it.

Sample Preparation. Samples of $[Fe_3O(O_2CCH_3)_6(4\text{-Me-py})_3](CHCl_3)$ and $[Fe_3O(O_2CCH_3)_6(4\text{-Me-py})_3](CDCl_3)$ were prepared as before.[9a] The nondeuterated sample for heat capacity measurements was originally prepared in two batches of 9 and 10 g. Before the heat capacity measurements were carried out, these two batches were combined and recrystallized in one batch by dissolution in $CHCl_3$, followed by slow evaporation. Anal. Calcd for $C_{31}H_{40}N_3O_{13}Cl_3Fe_3$: C, 39.76; H, 4.30; N, 4.49; Fe, 17.89; Cl, 11.36. Found: C, 39.61; H, 4.46; N, 4.29; Fe, 17.95; Cl, 11.30.

Results and Discussion

Structures and Valence Detrapping. The 298 K single-crystal X-ray structures of complexes **1** and **2** were reported in a very recent paper.[9a] Both have $R32$ symmetry at temperatures above their valence-detrapping phase transitions: above ~207 K for **1** and above ~93 K for **2**. Although considerable effort has been expended, it has *not* proved possible to determine the structures below these temperatures. Each Fe_3O molecule has a central μ_3-O^{2-}, which lies exactly in a plane with the three iron ions and three pyridine N atoms. Along the c axis of **1** and **2**, Fe_3O complexes and $CHCl_3$ solvate molecules occupy alternating sites of 32 symmetry. In both **1** and **2**, the –CH moiety is disordered on the C_3 axis above and below a triangle of Cl atoms.

Variable-temperature ^{57}Fe Mössbauer spectra were reported[9a] for **1**. At temperatures below ~150 K, there are two quadrupole-split doublets, one for Fe^{II} and the other Fe^{III} in an area ratio of 1:2, respectively. At ~160 K, a third doublet with characteristics the same as those for a valence-detrapped average doublet suddenly appears. In the range 160–193 K, the amount of this third doublet increases from 13.8 (1) to 25.2 (2)% of the spectra area. Throughout this temperature range, the components of the three doublets move together to become one "average-valence" doublet, a process which appears to be completed at ~208 K. This is approximately the temperature where a first-order phase transition was noted[9a] for **1**. Valence detrapping of the Fe_3O

(11) (a) Webb, R. J.; Rheingold, A. L.; Geib, S. J.; Staley, D. L.; Hendrickson, D. N. *Angew. Chem., Int. Ed. Engl.* **1989**, *28*, 1388. (b) Webb, R. J.; Geib, S. J.; Staley, D. L.; Rheingold, A. L.; Hendrickson, D. N. *J. Am. Chem. Soc.* **1990**, *112*, 5031.
(12) Cohn, M. J.; Timken, M. D.; Hendrickson, D. N. *J. Am. Chem. Soc.* **1984**, *106*, 6683.
(13) Chrisman, B. L.; Tumolillo, T. A. *Comput. Phys. Commun.* **1971**, *2*, 322.
(14) Sorai, M.; Kaji, K.; Kaneko, Y. *J. Chem. Thermodyn.* **1992**, *24*, 167.
(15) Ogasahara, K.; Sorai, M.; Suga, H. *Mol. Cryst. Liq. Cryst.* **1980**, *71*, 189.
(16) Wittebort, R. J.; Subramanian, R.; Kulshreshtha, N. P.; Du Pre, D. B. *J. Chem. Phys.* **1985**, *83*, 2457.

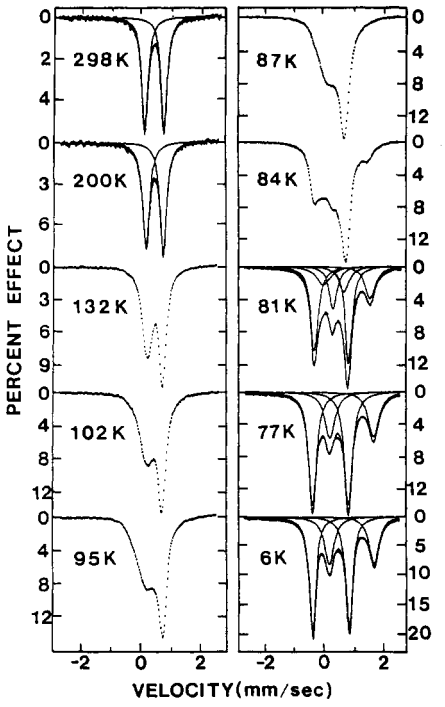

Figure 1. Variable-temperature ^{57}Fe Mössbauer spectra for $[Fe_3O(O_2CCH_3)_6(4\text{-Me-py})_3](CHCl_3)$ (**2**).

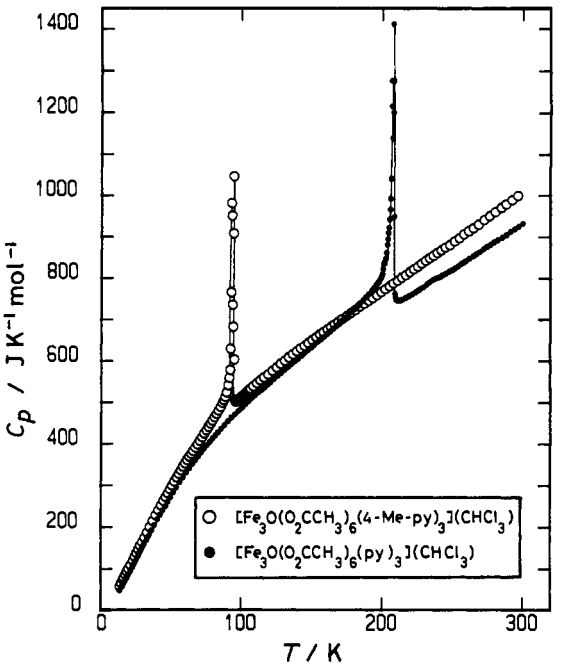

Figure 2. Heat capacity at constant pressure, C_p, versus temperature for $[Fe_3O(O_2CCH_3)_6(py)_3](CHCl_3)$ (**1**) and $[Fe_3O(O_2CCH_3)_6(4\text{-Me-py})_3](CHCl_3)$ (**2**).

complexes in **1** occurs cooperatively in a phase transition.

Mössbauer data for complex **2** are presented in Figure 1. In the case of several of these spectra, the features were least-squares-fit to Lorentzian line shapes. Fitting parameters are given in Table I. Complex **2** is valence trapped (two doublets in an area ratio of 2:1) on the Mössbauer time scale below 77 K. A third doublet characteristic of a valence-detrapped complex suddenly appears in the 81 K spectrum. At temperatures above this, the spectrum relatively abruptly changes to one doublet such that by 87–95 K there is only the valence-detrapped doublet present. Complex **2** converts from trapped to detrapped in a 15-deg range, whereas $[Fe_3O(O_2CCH_3)_6(py)_3](CHCl_3)$ was reported[9a] to make this change over a 70-deg range. Thus, complex **2** and isostructural $[Mn_3O(O_2CCH_3)_6(py)_3](py)$, which has been characterized[17] by solid-state ^{2}H NMR spectroscopy, make by far the most abrupt conversions from trapped to detrapped of all mixed-valence compounds.

It was decided that it is *not* appropriate to simulate the Mössbauer spectra shown in Figure 1 with a three-site (or four-site) relaxation model. Several reasons can be given as follows. A detailed analysis of the spectra for $[Fe_3O(O_2CCH_3)_6(py)_3]\cdot py$ has been presented[9e] to show that the temperature dependence of the Mössbauer spectrum is not consistent with a simple relaxation model. First, it was shown that in the 61–144 K region the spectra could be fit with three doublets (Fe^{III}, Fe^{II}, and valence detrapped) with quite reasonable line widths. Second, simulations of the Mössbauer spectra were carried out by employing a three-site relaxation model. These simulated spectra did *not* mimic well the temperature dependence seen.[9e] Third, from variable-temperature ^{2}H NMR data on an oriented single crystal of $[Fe_3O(O_2CCD_3)_6(py)_3]\cdot py$ it was definitively concluded that the rate of the process that averages the Fe^{III} and Fe^{II} valences in this complex is less than 3.1×10^4 s^{-1} at $\sim$173 K.[9d] Since the ^{57}Fe Mössbauer spectra for this complex show the rate of this valence detrapping process is greater than $\sim 10^9$ s^{-1} at $\sim$190 K (one doublet), a change from less than 3.1×10^4 s^{-1} to greater than $\sim 10^9$ s^{-1} in a $\sim$17-deg interval is not at all consistent with a simple relaxation model. In such a model it is tacitly assumed that for an individual molecule there is a potential energy diagram with barriers between different states. With an increase in temperature, the molecule is able to overcome the barriers and the rate of the interconversion process increases. However, it is clear that valence detrapping occurs cooperatively in phase transitions. There is a catastrophic event, and the kinetics are those of domain walls moving in the crystal, not individual molecules overcoming barriers. A dramatic example of just how abruptly valence detrapping can occur is found with $[Mn_3O(O_2CCH_3)_6(py)_3]\cdot py$.[17] A plot of the excess entropy gain versus temperature shows that $\sim$67% of the total entropy gain occurs in a $\sim$5-deg interval in a first-order phase transition that involves valence detrapping in the Mn_3O complex and the onset of motion of the pyridine solvate molecule.

Further evidence that "lattice dynamics" are determining the temperature dependence of the Mössbauer spectra of mixed-valence complexes is available. It has been shown[9h] that for $[Fe_3O(O_2CCH_3)_6(4\text{-Et-py})_3]\cdot 4\text{-Et-py}$ there is no evidence of relaxation effects in the Mössbauer spectra. Only two doublets are seen in each Mössbauer spectrum in the 6.5–298 K range. There is a valence-averaging process present. However, the Fe^{II} and Fe^{III} doublets just move together to become one average-valence doublet *without any evidence of line broadening*. These spectra do *not* need to be simulated by a relaxation model. If the rate of the valence-detrapping process is increasing with increasing temperature and goes through the range ($\sim 10^6$–10^9 s^{-1}) that should affect the line shapes of Mössbauer signals, line broadening and coalescence should be seen. They are not. The inescapable conclusion is that, whatever the process affecting the Mössbauer spectrum for the above complex, it is at all temperatures faster than the ^{57}Fe Mössbauer technique can sense. It was for the above reasons that we decided not to simulate the spectra of Figure 1 with a relaxation model, but to fit the spectra with Lorentzian line shapes.

Heat Capacity Measurements. Adiabatic calorimetric measurements were made on 16.3703 g of $[Fe_3O(O_2CCH_3)_6(4\text{-Me-py})_3](CHCl)_3$ in four series: series 1 (110–300 K), series 2 (78–109 K), series 3 (14–97 K), and series 4 (88–98 K). The results were evaluated in terms of C_p, the molar heat capacity at constant pressure. The C_p versus temperature data are listed in the supplementary material and plotted in Figure 2, where the C_p data for complex **1** are also shown for comparison purposes. Complex **2** exhibits reproducibly two C_p peaks in the phase-

(17) (a) Jang, H. G.; Vincent, J. B.; Nakano, M.; Huffman, J. C.; Christou, G.; Sorai, M.; Wittebort, R. J.; Hendrickson, D. N. *J. Am. Chem. Soc.* **1989**, *111*, 7778. (b) Nakano, M.; Sorai, M.; Vincent, J. B.; Christou, G.; Jang, H. G.; Hendrickson, D. N. *Inorg. Chem.* **1989**, *28*, 4608.

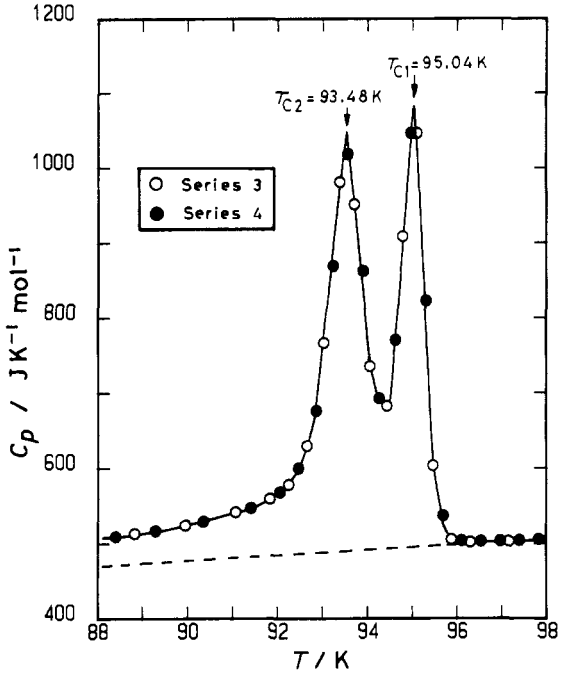

Figure 3. Molar heat capacity of $[Fe_3O(O_2CCH_3)_6(4\text{-Me-py})_3](CHCl_3)$ (**2**) in the vicinity of the phase-transition region. Two independent data sets (series 3 and 4) were run in this region. The broken curve indicates the normal heat capacity.

transition region at 93.48 K (T_{C2}) and 95.04 K (T_{C1}); see Figure 3. It is interesting to note that the other $CHCl_3$ solvate, complex **1**, was also found[9b] to exhibit two C_p peaks in the phase-transition region. For complex **1**, these two peaks were found at 207.14 K (T_{C2}) and 208.19 K (T_{C1}). In the paper[9b] describing the C_p measurements for complex **1**, it was suggested that perhaps the double-peak behavior was a reflection of the fact that the heat capacity sample of complex **1** was prepared in two batches. This cannot be the explanation for the double C_p peaks for complex **2**, for the heat capacity sample was recrystallized from $CHCl_3$ in one batch. Thus, it is clear that the double-C_p-peak behavior is an intrinsic feature to these two $CHCl_3$ solvates.

To determine the excess heat capacities due to the phase transitions from experimental C_p values, it is necessary to estimate a "normal" heat capacity curve. An effective frequency-distribution method[18] was employed. The effective frequency-distribution method assumes that the normal heat capacity of a solid arises from both a continuous phonon distribution and a number of discrete intramolecular vibrational modes. A borderline between them can be regarded as being 700 cm^{-1} for metal complexes such as complexes **1** and **2**. In the manner detailed[9b] for complex **1**, we employed IR and Raman data for complex **2** to characterize the discrete intramolecular vibrational modes of complex **2**. From C_p values in the ranges 13–40 and 120–270 K the "best" three effective frequency distributions below 700 cm^{-1} were determined by the least-squares method. Combination of each continuous spectrum below 700 cm^{-1} thus obtained and the discrete spectrum above 700 cm^{-1} forms a complete set of an effective frequency distribution, and each set gives a normal heat capacity curve. The normal heat capacity curve finally determined as an average of the three normal C_p curves is shown by a broken line in Figure 3.

The difference between the observed and normal heat capacities is the excess heat capacity, ΔC_p, due to phase transitions. The enthalpy (ΔH) and entropy (ΔS) arising from the phase transition were determined by integration of ΔC_p with respect to T and ln T, respectively. The values of ΔH and ΔS averaged over three normal C_p curves are ΔH = 1511 ± 111 J mol^{-1} and ΔS = 17.18 ± 1.42 J K^{-1} mol^{-1}.

(18) Sorai, M.; Seki, S. *J. Phys. Soc. Jpn.* **1972**, *32*, 382.

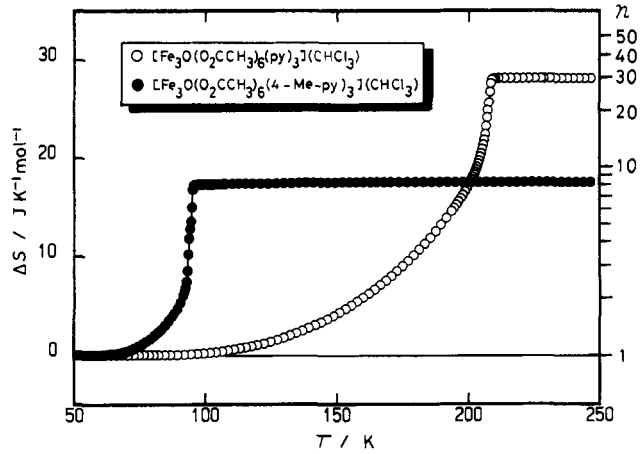

Figure 4. Acquisition of the transition entropy as a function of temperature for complexes **1** and **2**.

A plot of ΔS versus temperature for complex **2** is shown in Figure 4, where ΔS data from the literature[9b] are also plotted for complex **1**. The total ΔS = 28.10 ± 0.44 J K^{-1} mol^{-1} observed for complex **1** is considerably larger than the ΔS measured in this work for complex **2**. The ΔS value for complex **1** is close to R ln 32 (=28.82 J K^{-1} mol^{-1}) and has been attributed[9b] to two sources. When each Fe_3O complex in **1** converts from being statically trapped in one vibronic state to dynamically interconverting between four vibronic states, this contributes R ln 4 to ΔS. It has been shown[9a] for complex **1** that coupled to this valence detrapping is the onset of motion of the $CHCl_3$ solvate molecule between eight distinguishable lattice sites. This onset of motion of the $CHCl_3$ contributes R ln 8, which gives a total of R ln 4 + R ln 8 = R ln 32.

The smaller value of ΔS observed for complex **2** is also understandable if it is noted that the experimental ΔS value is quite close to R ln 8 (=17.29 J K^{-1} mol^{-1}). This leads to a proposal as to what events are occurring cooperatively in the double C_p peak phase transition of complex **2**. It seems reasonable to suggest that the Fe_3O complexes in **2** also valence-detrap and interconvert dynamically between four vibronic states to contribute R ln 4. In contrast to the case of complex **1**, we suggest that the $CHCl_3$ solvate molecules only begin to jump between two positions in the phase transition of complex **2**. Thus, the chloroform C–H vector only begins to jump between two positions, one "up" and the other "down" along the C_3 axis (c axis of $R32$). For complex **1**, the chloroform C–H vector jumps between eight positions, four up and four down. The four "up" positions consist of one on the c axis and three equally spaced on a cone off the c axis.

Solid-State ^{2}H NMR Spectroscopy. The ^{2}H nucleus has I = 1 and therefore a quadrupole moment which interacts with an asymmetric electronic charge distribution, the electric field gradient. If a single crystal is held fixed in a magnetic field and there is only one type of deuteron site in the crystal, the allowed ($\Delta m_I = \pm 1$) NMR transitions give rise to a quadrupole-split doublet, where the splitting is a projection on the magnetic field direction of the quadrupole coupling of the nuclear and electronic charge moments. If α is the angle between the C–D vector and the external magnetic field, then the quadrupolar splitting observed ($\Delta\nu_q$) is given by eq 1. If the temperature of a fixed sample (e.g.,

$$\Delta\nu_q(\alpha) = \tfrac{3}{2}[(e^2qQ/h)(3\cos^2\alpha - 1)/2] \qquad (1)$$

single crystal) is increased and the part of the molecule where the ^{2}H nucleus resides begins to become dynamic in the solid, then the quadrupole splitting will be reduced in magnitude by this motion. If the deuteron site tumbles freely in the solid at some elevated temperature, then the quadrupole splitting goes to zero. Solid-state ^{2}H NMR spectroscopy is particularly well suited for characterizing the onset of solvate molecule motion in these Fe_3O complexes.[9a,c,d]

In addition to the quadrupolar coupling, there is a second type of interaction in evidence in the ^{2}H NMR spectra of Fe_3O com-

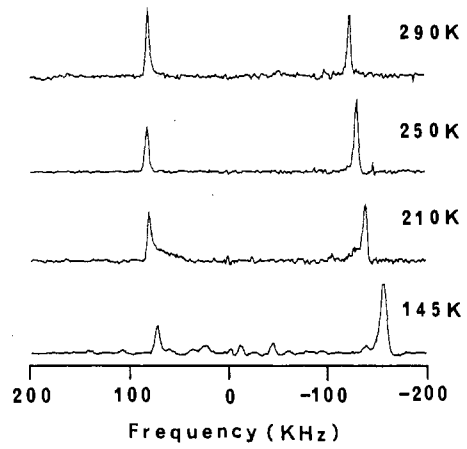

Figure 5. Temperature dependence of the solid-state ^2H NMR spectra of a magnetically oriented collection of ~20 small crystals of $[Fe_3O(O_2CCH_3)_6(4\text{-Me-py})_3](CDCl_3)$ (**2**) in eicosane. The external magnetic field is oriented parallel to the *c* axis of the crystals. The signs of the shifts are reversed from the usual convention.

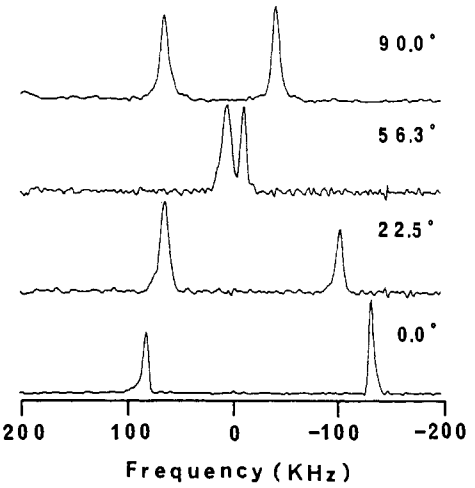

Figure 6. ^2H NMR spectra of magnetically oriented collection of ~20 small crystals of $[Fe_3O(O_2CCH_3)_6(4\text{-Me-py})_3](CDCl_3)$ at 250 K. The angle given for each spectrum is the angle between the magnetic field and the crystallographic *c* axis. The signs of the shifts are reversed from the usual convention. That is, shifts to negative frequency values correspond to downfield shifts.

plexes. The $Fe^{II}Fe^{III}_2$ complexes are paramagnetic with a $S = 1$ ground state. In the 50–300 K range, not only this ground state but several excited states with $S = 0$ to $S = 7$ are thermally populated. The magnetic exchange interaction between pairs of high-spin Fe^{II} and Fe^{III} ions is of the order of 10–50 cm^{-1}. The magnetic moment associated with the unpaired electrons of a neighboring Fe_3O complex interacts with the magnetic moment of a ^2H nucleus on the solvate molecule. This through-space dipolar interaction imparts a chemical shift to the quadrupole-split doublet, shifting it off the zero of frequency, which would be found for a diamagnetic compound.

Approximately 20 small crystals of $[Fe_3O(O_2CCH_3)_6(4\text{-Me-py})_3](CDCl_3)$ were magnetically oriented in fluid eicosane which was then cooled to room temperature to form a wax cube. In the cube, all the crystals have their principal axes of the magnetic susceptibility tensor aligned. From previous studies[9a,c,d,e] it is known that the principal axis corresponds to the crystallographic *c* axis (C_3 axis), along which the Fe_3O and $CHCl_3$ molecules occupy alternating sites of 32 symmetry. ^2H NMR spectra were obtained at various temperatures with the above eicosane cube oriented so that the magnetic field is oriented along the *c* axis of the $[Fe_3O(O_2CCH_3)_6(4\text{-Me-py})_3](CDCl_3)$ crystals; see Figure 5. A single quadrupole-split doublet is seen at all temperatures down to 145 K. The motion-modulated quadrupole splitting of the doublet, $\overline{\Delta\nu_q}$, gradually increases as the temperature is decreased: 206 kHz at 290 K; 213 kHz at 250 K; 220 kHz at 210 K; 226 kHz at 175 K; and 232 kHz at 145 K. It is unfortunate that we could not decrease the temperature to that of the phase transition. There are two important points to make relative to the observed temperature dependence of $\overline{\Delta\nu_q}$. First, the value of $\Delta\nu_q(0°)$ reported[19] for static (frozen) $CDCl_3$ is 244 kHz. Thus, as the temperature is decreased, the motion of $CDCl_3$ in the crystals of complex **2** is slowing down, and at 145 K the observed value of $\overline{\Delta\nu_q} = 232$ kHz is close to that for static $CDCl_3$. Indeed, a plot of $\overline{\Delta\nu_q}$ versus temperature gives a straight line that, when extrapolated to low temperature, intercepts the expected static splitting value of 244 kHz at ~80 K. This temperature is quite close to the 94 K phase-transition temperature.

Second, the reported[9a] temperature dependence of $\overline{\Delta\nu_q}$ for a magnetically oriented collection of crystals of complex **1**, i.e., $[Fe_3O(O_2CCH_3)_6(py)_3](CDCl_3)$, is different from that observed for complex **2**. Above the ~208 K valence-detrapping phase transition of complex **1**, the value of $\Delta\nu_q$ remains relatively constant at 196–204 kHz in the 295–223 K range. When the sample temperature of complex **1** is decreased below ~208 K, the value of $\overline{\Delta\nu_q}$ *decreases*: 170 kHz at 193 K; 160 kHz at 153 K; and 144 kHz at 110 K. The temperature dependence of $\overline{\Delta\nu_q}$ above the ~208 K phase transition was attributed to the C–D vector jumping between four positions of equal probability. (Actually, there are eight positions, four up and four down; however there is no change in $\overline{\Delta\nu_q}$ as a result of averaging about a C_2 axis which is perpendicular to the C_3 axis.) Of the four up positions, one is where the C–D vector is along the C_3 axis and the other three were calculated to be equally spaced on a cone with an angle $\alpha = 24.7°$ at 295 K. The decrease in $\overline{\Delta\nu_q}$ for complex **1** from 193 to 110 K was explained by proposing that the motion of the chloroform solvate slows down in this range. Also, each Fe_3O molecule becomes valence trapped and distorted where the two Fe^{II}–Fe^{III} bond lengths are appreciably larger than the Fe^{III}–Fe^{III} bond length. Thus, the motion of the $CDCl_3$ ceases with the C–D vector pointed off the C_3 axis. At 110 K, the observed quadrupole splitting was used[9a] to calculate $\alpha = 31.5°$ for the *one* position into which the C–D vector becomes statically fixed. The C–D vector comes to rest off the C_3 axis, pointing at the Fe^{II} ion for complex **1**.

In the case of complex **2**, the increase in $\overline{\Delta\nu_q}$ as the crystal is cooled in the 290–145 K range indicates that the C–D vector is rapidly precessing around the C_3 axis at some angle α and this angle approaches zero as the temperature is cooled to the ~94 K phase-transition temperature. The fact that the C–D vector is moving about the C_3 axis in the 145–290 K range is established in the following manner. In Figure 6 are shown ^2H NMR spectra obtained at 250 K where the wax cube was turned so that the angle between the magnetic field and the principal axis of the magnetic susceptibility tensor is changed from 0 to 90.0°. As the goniometer angle is increased from 0°, the quadrupole splitting of the doublet gradually decreases. It should become zero at the magic angle (54.7°), where $3\cos^2\alpha - 1 = 0$. When $\alpha = 90°$, the quadrupole splitting is seen to be 108 kHz at 250 K, which is exactly half the value obtained in the 0° spectrum. Thus, the C–D vector is in motion about the C_3 axis and the motion is axially symmetric. If we assume that the C–D chloroform vector in complex **2** experiences equally the same four up positions as described for the $CDCl_3$ of complex **1**, then for complex **2** we can calculate for the three off-C_3-axis positions $\alpha = 18.5°$ at 290 K and this gradually decreases to $\alpha = 10°$ at 145 K.

In addition to the temperature dependence of quadrupole splitting, the ^2H NMR spectra of complexes **1** and **2** also differ in the temperature dependence of chemical shifts. It was reported[9a] for complex **1** that the ^2H doublet is shifted 706 ppm to low field above the ~208 K phase transition and below this temperature

(19) Kunwar, A. C.; Gutowsky, H. S.; Oldfield, E. *J. Magn. Reson.* **1985**, *62*, 521.

the doublet shifts to lower field such that the chemical shift is 2228 ppm downfield at 100 K. These measurements were made with the magnetic field oriented along the C_3 axis of the crystals. As can be seen in Figure 5 where the frequencies are reversed from the usual convention, decreasing the temperature of the parallel-oriented wax cube of complex **2** from 290 to 145 K leads to a downfield shift of the $CDCl_3$ doublet. At 290 K, the doublet is shifted 20 kHz downfield, which at 38.8 MHz corresponds to a 516 ppm downfield chemical shift. At 210 K, the shift is 645 ppm downfield, and this increases to a 1032 ppm downfield shift at 145 K. The magnitude of the chemical shift varies linearly with reciprocal temperature, thus showing that the local paramagnetic field from neighboring Fe_3O complexes has simple Curie law behavior to 145 K, which is well above the 94 K transition temperature at which the molecule undergoes substantial structural and electronic rearrangement. These are large chemical shifts, and previously in a closely related cluster with a pyridine solvate molecule we observed[9e] solvate ^2H shifts of approximately half the magnitude seen here, which were attributed to a through-space dipolar coupling. Two facts indicate that the shifts reported here are of the same type. First, the orientation dependence of the shift (Figure 6) shows that the paramagnetic coupling is predominantly anisotropic ($\Delta\sigma$ = 1550 ppm at 145 K) with no measurable isotropic shift at the resolution of these experiments (30 ppm). Direct contact interactions are typically dominated by an isotropic shift. Second, for the complex with the pyridine solvate molecule, we estimated from the X-ray structure that the average distance between solvate deuterons and Fe atoms is 5.7 Å.[9e] From the X-ray structures we estimate that the chloroform deuteron is substantially closer, ~4.0 Å for **1** or ~4.1 Å for **2**. Since the dipolar coupling varies with $1/r^3$, the closer approach of the chloroform deuterons qualitatively accounts for the substantially larger chemical shifts. The 2228 ppm shift observed for **1** at 100 K (valence trapped) as compared to the 1032 ppm shift for **2** at 145 K (valence detrapped) results both from the different solvate geometries and from the difference in the local fields. Regardless of the details, ^2H NMR spectroscopy clearly shows that the $CDCl_3$ solvate molecules are behaving differently in complexes **1** and **2**.

Concluding Comments. In spite of the fact that $[Fe_3O(O_2CCH_3)_6(py)_3](CHCl_3)$ (**1**) and $[Fe_3O(O_2CCH_3)_6(4\text{-Me-py})_3](CHCl_3)$ (**2**) are isostructural, the chloroform solvate molecules exhibit intriguing differences in their influence on intramolecular electron transfer in the Fe_3O complexes **1** and **2**. In the case of the py complex, the $CHCl_3$ solvate structure contributes $\sim R$ ln 8 to ΔS for the cooperative valence detrapping. In this case, the chloroform C–H moiety interacts with the underside of a Fe_3O complex and four potential energy minima result. In complex **1**, the chloroform solvate molecule jumps between these four positions. There are potential energy barriers between these four orientations. At the ~208 K phase transition, each $CHCl_3$ in complex **1** converts from being statically locked in one position to jumping between eight distinguishable crystal sites.

The case for the $CHCl_3$ solvate molecules in complex **2** is quite different. With the assumption that valence detrapping in the Fe_3O complexes contributes R ln 4 to the entropy gain, the heat capacity results show that the $CHCl_3$ molecules only contribute $\sim R$ ln 2 to ΔS for the phase transition at ~94 K. This implies that the only motion of the $CHCl_3$ solvate molecule which couples to the valence-detrapping phase transition is that where the C–H vector goes from being static to jumping between the "up" and "down" positions along the C_3 axis. However, the ^2H NMR results also show that the chloroform C–H vector is moving axially about the C_3 axis for complex **2** above the ~94 K phase-transition temperature. A possible explanation for why the solvate molecule in complex **2** only contributes $\sim R$ ln 2 to the transition entropy can be gleaned from a comparison of the 298 K X-ray structures[9a] of **1** and **2**. Complex **2** has a shorter stacking axis (c axis) of 10.373 (3) Å compared to 10.488 (3) Å for complex **1**. This means obviously that the solvate cavity which holds one $CHCl_3$ molecule is smaller for complex **2**. However, the a-axis (≡b-axis) dimension of 18.759 (6) Å for **2** is appreciably larger than the 17.819 (6) Å value for **1**. The 4-methyl substituents on the pyridine ligands in **2** lead to the pyridine–pyridine contacts between Fe_3O complexes becoming weaker in **2** compared to **1**. It is this weaker intermolecular interaction between neighboring Fe_3O complexes that leads to a lower temperature for the phase transition for **2** than for **1**.

In the case of complex **2**, the phase transition occurs at a low temperature of ~94 K. The Fe_3O complexes valence-detrap cooperatively because the thermal energy breaks down the (4-Me-py)···(4-Me-py) intermolecular contacts. Because the c axis is so small for complex **2** at this temperature, the only thing the $CHCl_3$ solvate molecules can do cooperatively is to begin flipping head-to-tail. As the temperature of complex **2** is further increased above ~94 K, the chloroform C–H vector does start to move off the C_3 axis on a cone. There are probably three positions of minimum potential energy for the C–H vector moving on the cone. The C–H vector may, in fact, jump between these three minima as it apparently does in complex **1**. Entropy is gained, however, very gradually for this $CHCl_3$ jumping in complex **2**. This is the case because there is no cooperativity associated with the off-C_3-axis $CHCl_3$ motion for **2** above ~94 K. At ~94 K, all long-range order is destroyed for complex **2** and each $CHCl_3$ molecule has no way to communicate with other $CHCl_3$ molecules. On the other hand, the py···py intermolecular interaction is greater in complex **1** and a higher temperature of ~208 K is required for the phase transition. At this temperature, the c axis of **1** is sufficiently large not only to permit the $CHCl_3$ molecules to jump head-to-tail but also to permit the C–H vectors to *cooperatively* jump to sites off the C_3 axis. Thus, the $CHCl_3$ solvate molecule of **1** contributes $\sim R$ ln 8 to ΔS, whereas the $CHCl_3$ molecule of **2** only contributes $\sim R$ ln 2.

It is important to note that, in all $R32$ symmetry Fe_3O complexes which are thoroughly characterized, when rapid electron transfer occurs in the solid state, it is always the case that the solvate molecules present a C_3 symmetry environment about each Fe_3O complex. The interactions between a given Fe_3O complex and its two neighboring solvate molecules are probably very weak (10–100 cm^{-1}). However, they may be strong enough to modify the ground-state potential energy surface for the Fe_3O complex. In an asymmetric environment, the complex will be valence trapped in one minimum, e.g., $Fe_a^{II}Fe_b^{III}Fe_c^{III}$. Because of the mismatch in energy between this one minimum and others on the surface, the complex cannot tunnel to another state such as $Fe_a^{III}Fe_b^{II}Fe_c^{III}$. Molecular mechanics calculations are needed in order to describe the potential energy surface for motion of solvate molecules in these crystals. Also, further careful changes in the solvate molecule and the architecture of the Fe_3O complex are needed.

Finally, we note that we have not presented an explanation for the double-C_p-peak appearance observed for the phase transitions of both complexes **1** and **2**. It is clear that this is an intrinsic feature of these two $CHCl_3$ solvates. Neither of the two theoretical treatments[20,21] of the phase transitions observed for these $Fe^{II}Fe^{III}_2$ complexes accounts for the influence of the solvate molecules. It should be remarked, however, that the double-C_p-peak appearance has precedent in the literature. For example, the low-temperatue first-order phase transition of $[Fe_3O(O_2CCH_3)_6(py)_3]py$ has been reported[9g] to show two C_p peaks at 111.4 and 112.0 K. The origin of these two closely spaced C_p peaks in this pyridine solvate is probably the same as for the two $CHCl_3$ solvates **1** and **2**. A very thoroughly studied example of two closely spaced C_p peaks is found with $NaNO_2$, where two C_p peaks have been reported[22] to occur at 436.5 and 437.8 K. Through detailed studies it has been shown that $NaNO_2$ is in a ferroelectric phase III at room temperature and undergoes a phase transition at 436.5 K to an antiferromagnetic phase II, followed by a phase transition at 437.8 K to a paraelectric phase I. Thus, the antiferromagnetic phase II is stable at atmospheric pressure for only 1.3 K. Yamada et al.[23]

(20) Stratt, R. M.; Adachi, S. H. *J. Chem. Phys.* **1987**, *86*, 7156.
(21) Kambara, T.; Hendrickson, D. N.; Sorai, M.; Oh, S. M. *J. Chem. Phys.* **1986**, *85*, 2895.
(22) Sakiyama, M.; Kimoto, A.; Seki, S. *J. Phys. Soc. Jpn.* **1965**, *20*, 2180.

attributed the antiferroelectric character of phase II to a sinusoidal modulation of the electric moments of the NO_2^- ions along the *a* axis of the crystal. Hoshino and Motegi[24] deduced from X-ray diffraction data that the period of the sinusoidal modulation along the *a* axis drops from $\sim 10a_0$ to $\sim 8a_0$ in the narrow region of existence of phase II of $NaNO_2$.

It is clear that the $CHCl_3$ solvates **1** and **2** each undergo two phase transitions within a narrow temperature range. For each complex there is a phase which exists in a narrow temperature region. The orientations of $CHCl_3$ molecules along each stack could come into play in characterizing this phase. In the low-temperature phase, the C-H vectors of the $CHCl_3$ molecules could each be pointed in the same direction. In the high-temperature phase, the C-H vectors are reorienting rapidly. In the intermediate-temperature phase, which exists in a narrow temperature range, there could be a sinusoidal modulation of the orientation of C-H vectors.

Acknowledgment. We are grateful for support from National Institutes of Health Grant HL 13652 (D.N.H.) and National Science Foundation Grants DMB8606358 (R.J.W.) and CHE-9115286 (D.N.H.). M.S. and D.N.H. are also grateful for a travel grant from the National Science Foundation (INT-9016821) and the Japan Society for the Promotion of Science.

Supplementary Material Available: A table of molar heat capacities for compound **2** (3 pages). Ordering information is given on any current masthead page.

(23) Yamada, Y.; Shibuya, I.; Hoshino, S. *J. Phys. Soc. Jpn.* **1963**, *18*, 1594.
(24) Hoshino, S.; Motegi, H. *Jpn. J. Appl. Phys.* **1967**, *6*, 708.

Contribution from the Department of Chemistry, University of Massachusetts, Amherst, Massachusetts 01003

Reinvestigation of the Reaction of Triphenylphosphine with Tetracyanoethylene. Molecular Structure of *N*-(Heptacyanocyclopent-1-enyl)triphenylphosphoranimine

T. Mohan, Roberta O. Day, and Robert R. Holmes*

Received December 10, 1991

The reaction of triphenylphosphine with tetracyanoethylene was reported to give the compound with the formula $C_{30}H_{15}N_8P$ on the basis of elemental analysis. The reaction was repeated and the composition confirmed by X-ray crystallography. However, the proposed phosphole ring structure containing pentacoordinated phosphorus was shown to be erroneous. Conclusive proof is provided from X-ray analysis that the product is a phosphoranimine containing the $Ph_3P{=}N$ unit.

Introduction

Very little is known about the conformational requirements of five-membered rings in pentacoordinated phosphorus-carbon heterocycles compared to that known for the corresponding cyclic oxyphosphoranes.[1-3] This may be due to the unavailability of general feasible synthetic routes for such compounds, but more likely it is due to the decreased stability of these compounds brought about by a buildup of charge at phosphorus caused by the attachment of carbon ligands of reduced electronegativity.

Earlier, Reddy and Weiss[4] had reported that the reaction of triphenylphosphine with dicyanoacetylene and tetracyanoethylene produced phosphoranes containing phosphole rings, formulated as A and B, respectively. Tebby et al.[5] reinvestigated the former reaction and, on the basis of their data, concluded that the product formed was not a phosphole as represented by A but rather the acyclic derivative C, an alkene-1,6-diylidenediphosphorane. Their study[5] suggested that the reaction leading to the product formulated as B[4] also was suspect and prompted us to reinvestigate the reaction of Ph_3P with tetracyanoethylene. The results are the focus of this paper.

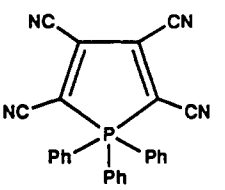

A

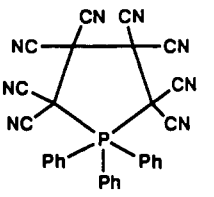

B

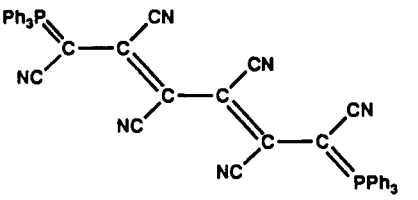

C

Experimental Section

All experiments were carried out in an atmosphere of dry nitrogen. Tetracyanoethylene and triphenylphosphine (Fluka) were used as such. Acetonitrile and methylene chloride were distilled by conventional methods before use.[6]

An infrared spectrum was recorded on a Perkin-Elmer 783 spectrophotometer as a Nujol mull using NaCl windows. The $^{31}P(^1H)$ NMR spectrum was recorded on a Varian XL-300 (121.5-MHz) spectrometer as a $CDCl_3$ solution using 85% H_3PO_4 as the external standard. Chemical shift values (δ in ppm) were assigned negative values when the signals were upfield relative to H_3PO_4. The melting point was uncorrected.

Crystallography. The X-ray crystallographic study was done by using an Enraf-Nonius CAD4 diffractometer and graphite-monochromated molybdenum radiation ($\lambda(K\alpha_1) = 0.709\,30$ Å, $\lambda(K\alpha_2) = 0.713\,59$ Å) at an ambient temperature of 23 ± 2 °C. Details of the experimental and computational procedures have been described previously.[7]

Synthesis of *N*-(Heptacyanocyclopent-1-enyl)triphenylphosphoranimine, $Ph_3PNC_5(CN)_7$ (1). To a stirred suspension of tetracyanoethylene (1.95 g, 15.3 mmol) in CH_3CN (20 mL) at 0 °C (ice bath) was added in ca. 1 h triphenylphosphine (2.0 g, 7.6 mmol) dissolved in CH_3CN (30

(1) Kumara Swamy, K. C.; Burton, S. D.; Holmes, J. M.; Day, R. O.; Holmes, R. R. *Phosphorus, Sulfur, Silicon* **1990**, *53*, 437 and references cited therein.
(2) Kumara Swamy, K. C.; Day, R. O.; Holmes, J. M.; Holmes, R. R. *J. Am. Chem. Soc.* **1990**, *112*, 6095.
(3) Burton, S. D.; Kumara Swamy, K. C.; Holmes, J. M.; Day, R. O.; Holmes, R. R. *J. Am. Chem. Soc.* **1990**, *112*, 6104.
(4) Reddy, G. S.; Weiss, C. D. *J. Org.Chem.* **1963**, *28*, 1822.
(5) Shaw, M. A.; Tebby, J. C.; Ward, R. S.; Williams, D. H. *J. Chem. Soc. C* **1968**, 1609.
(6) Perrin, D. D.; Armanego, W. L. F.; Perrin, D. R. *Purification of Laboratory Chemicals*, 2nd ed.; Pergamon Press: Oxford, U.K. 1980.
(7) Sau, A. C.; Day, R. O.; Holmes, R. R. *Inorg. Chem.* **1981**, *20*, 3076.

0020-1669/92/1331-2271$03.00/0